



# Inhibition of monoamine oxidase by C5-substituted phthalimide analogues

Clarina I. Manley-King, Jacobus J. Bergh, Jacobus P. Petzer\*

Pharmaceutical Chemistry, School of Pharmacy, North-West University, Private Bag X6001, Potchefstroom 2520, South Africa

## ARTICLE INFO

### Article history:

Received 20 May 2011

Revised 20 June 2011

Accepted 26 June 2011

Available online 29 June 2011

### Keywords:

Monoamine oxidase

Reversible inhibition

Phthalimide

Isatin

Molecular docking

## ABSTRACT

Literature reports that isatin as well as C5- and C6-substituted isatin analogues are reversible inhibitors of human monoamine oxidase (MAO) A and B. In general, C5- and C6-substitution of isatin leads to enhanced binding affinity to both MAO isozymes compared to isatin and in most instances result in selective binding to the MAO-B isoform. Crystallographic and modeling studies suggest that the isatin ring binds to the substrate cavities of MAO-A and -B and is stabilized by hydrogen bond interactions between the NH and the C2 carbonyl oxygen of the dioxindolyl moiety and water molecules present in the substrate cavities of MAO-A and -B. Based on these observations and the close structural resemblances between isatin and its phthalimide isomer, a series of phthalimide analogues were synthesized and evaluated as MAO inhibitors. While phthalimide and *N*-aryl-substituted phthalimides were found to be weak MAO inhibitors, phthalimide homologues containing C5 substituents were potent reversible inhibitors of recombinant human MAO-B with IC<sub>50</sub> values ranging from 0.007 to 2.5  $\mu$ M and moderately potent reversible inhibitors of recombinant human MAO-A with IC<sub>50</sub> values ranging from 0.22 to 9.0  $\mu$ M. By employing molecular docking the importance of hydrogen bonding between the active sites of MAO-A and -B and the phthalimide inhibitors are highlighted.

© 2011 Elsevier Ltd. All rights reserved.

## 1. Introduction

Monoamine oxidase A and B (MAO-A and -B) are flavin adenine dinucleotide (FAD)-containing enzymes which are attached to the outer membrane of mitochondria.<sup>1</sup> The FAD cofactors are covalently bound to the MAO enzymes via a thio ether linkage between the side chain of a cysteinyl residue and the C8 $\alpha$ -position of the FAD.<sup>2</sup> In both MAO isoforms this cysteine residue is part of the conserved pentapeptide Ser-Gly-Gly-Cys-Tyr. Even though MAO-A and -B are encoded by different genes, they share approximately 70% amino acid sequence identity.<sup>3</sup> Both MAO genes are located on the X chromosome and consist of 527 and 520 amino acids, respectively. These findings, together with observation that the genes exhibit identical exon-intron organizations, suggest that the two isoforms are derived from a common ancestral gene.<sup>3,4</sup>

The MAO genes are expressed in a variety of central and peripheral tissues including the liver, brain, blood platelets, placenta and gastrointestinal tract. Within these tissues the concentrations and activities of the MAO's differ. MAO-B activity is found almost exclusively in human blood platelets<sup>5</sup> while MAO-A activity is exclusively present in the human placental<sup>6</sup> and gut tissues.<sup>7</sup> Within the human liver, MAO-B is the most abundant isoform.<sup>8</sup> Both MAO isoforms are found in the human brain, although they are differently distributed<sup>9</sup> with MAO-B present in higher levels.<sup>10,11</sup>

Of particular interest is the observation that MAO-B is the most abundant form in the human basal ganglia.<sup>11,12</sup>

The principal biochemical function of the MAO's is thought to be the catalysis of the  $\alpha$ -carbon oxidation of a variety of monoamine neurotransmitters and dietary amines. In addition the MAO's also oxidize amine containing xenobiotic drugs and toxins. For example, serotonin acts as the preferential substrate for MAO-A while the false neurotransmitters, benzylamine and  $\beta$ -phenylethylamine, are selectively oxidized by MAO-B.<sup>13,14</sup> Dopamine, epinephrine and norepinephrine are substrates for both isoforms.<sup>14,15</sup> These observations suggest that the MAO's do not only function to terminate the central action of neurotransmitter amines, but may also protect neurons from stimulation by extraneous amines by degrading false neurotransmitters.<sup>3</sup> The MAO's have also been shown to activate neurotoxins. For example, the central oxidation and subsequent activation of the parkinsonian inducing pro-neurotoxin, 1-methyl-4-phenyl-1,2,3,6-tetrahydropyridine (MPTP), is dependent upon the action of MAO-B.<sup>16</sup> In vitro experiments have shown that MPTP is a substrate for both isoforms. The MAO-A isoform, however, is rapidly inactivated by reactive intermediates which form when MPTP is oxidized by MAO-A and therefore does not significantly contribute to the oxidation of MPTP in vivo.<sup>16</sup>

The location of MAO-A and -B in the brain and its role in the degradation of monoamine neurotransmitters have made these enzymes attractive targets for the development of drugs for the treatment of neuropsychiatric and neurodegenerative diseases. For example, reversible and irreversible inhibitors of MAO-A are used to treat anxiety disorder and depression. Based on the

\* Corresponding author. Tel.: +27 18 2992206; fax: +27 18 2994243.

E-mail address: [jacques.petzer@nwu.ac.za](mailto:jacques.petzer@nwu.ac.za) (J.P. Petzer).

monoamine hypothesis of depression, MAO-A inhibitors reduce the degradation of serotonin, norepinephrine and dopamine in the brain which leads to increased levels of these neurotransmitters in the brain and a resulting antidepressant effect.<sup>14</sup> MAO-A inhibitors are particularly useful in the management of depression in elderly patients.<sup>14,17</sup> MAO-B inhibitors are currently clinically used in the treatment of Parkinson's disease. Since MAO-B appears to be primarily responsible for dopamine catabolism in the basal ganglia,<sup>12,18</sup> inhibitors may conserve the depleted dopamine supply in this brain region, enhance the concentration of dopamine that is derived from administered levodopa, the metabolic precursor of dopamine and prolong the action of dopamine.<sup>19,20</sup> Based on these observations, MAO-B inhibitors are frequently combined with levodopa in the therapy of Parkinson's disease.<sup>21</sup> Also of importance is the observation that MAO-B levels and activity increase in most brain regions, including the basal ganglia, with age.<sup>11,22,23</sup> In contrast, MAO-A activity remains constant with age.<sup>10</sup> Considering that Parkinson's disease occurs primarily in elderly patients, the age-associated increase of MAO-B and the consequent increase of MAO-B catalyzed dopamine turnover make MAO-B inhibitors particularly relevant in Parkinson's disease therapy. Of importance is the observation that in the primate brain, MAO-A also contribute to the catabolism of dopamine. For example, the selective irreversible inhibitor of MAO-A, clorgyline, is reported to enhance the concentration of dopamine in the striatum of primates treated with levodopa and the degree of this elevation is comparable to that obtained with (*R*)-deprenyl, a selective irreversible inhibitor of MAO-B.<sup>19</sup> Nonselective MAO-A/B inhibitors may therefore be more efficacious in prolonging the effect of dopamine in the basal ganglia.<sup>15</sup>

A significant disadvantage of MAO-A inhibition is the occurrence cardiovascular effects when combined with indirectly acting sympathomimetic amines such as tyramine which is present in certain foods.<sup>15,24</sup> This interaction occurs because tyramine is normally metabolized by MAO-A in the gut wall which reduces the amounts of tyramine that enters the systemic circulation. Irreversible inhibition of MAO-A prevents the normal catabolism of tyramine in the gut and hence leads to increased systemic concentrations of tyramine. In contrast, this interaction does not occur with reversible inhibitors since the inhibitor is readily displaced by tyramine which is subsequently normally metabolized by MAO-A. These observations suggest that when designing MAO-A selective inhibitors or MAO-A/B mixed inhibitors, the inhibitors should interact reversibly with MAO-A. Another advantage of reversible inhibition is that, following withdrawal of the drug, enzyme activity is recovered quickly upon elimination of the drug from the tissues. In contrast, after terminating treatment with irreversible MAO inhibitors, recovery of enzyme activity may require several weeks since the turnover rate for the biosynthesis of MAO in the human brain may be as much as 40 days.<sup>25</sup>

For these reasons several studies are underway to discover new MAO inhibitors which bind reversibly to the enzymes. An example of a reversible MAO-A/B mixed inhibitor is isatin (**1**) (Fig. 1). Isatin is an endogenous small molecule which inhibits both human MAO-A and -B with enzyme-inhibitor dissociation constants ( $K_i$  values) of 15  $\mu$ M and 3  $\mu$ M for the two isozymes, respectively.<sup>26</sup> While the X-ray crystal structure of isatin bound to MAO-A has not yet been determined, the three-dimensional structure of isatin complexed within the active site of recombinant human MAO-B is known.<sup>27</sup> The structure model shows that isatin is bound within the substrate cavity of MAO-B with the C2 carbonyl oxygen of the dioxindolyl moiety directed towards the FAD cofactor. Here the NH and the C2 carbonyl oxygen of isatin are stabilized by hydrogen bonding to water molecules present in the substrate cavity of MAO-B.<sup>27</sup> Of interest is the observation that with isatin located in the MAO-B substrate cavity, the entrance cavity of the

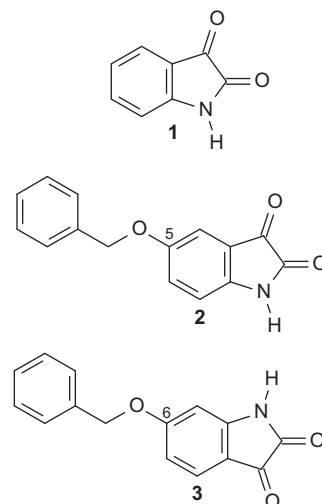


**Figure 1.** The structures of isatin (**1**), 5-benzyloxyisatin (**2**) and 6-benzyloxyisatin (**3**).

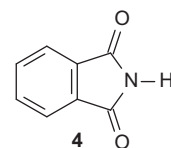


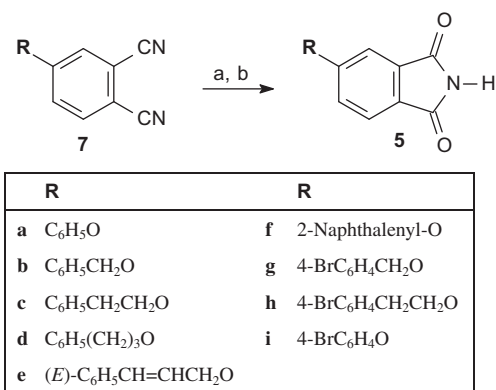
**Figure 2.** The structure of phthalimide (**4**).

enzyme is unoccupied. Based on this observation and modeling studies C5- and C6-substituted isatin analogues were previously examined as potential inhibitors of recombinant human MAO-A and -B.<sup>28,29</sup> In general, the isatin analogues proved to be potent and selective MAO-B inhibitors with selected members also exhibiting high binding affinities towards MAO-A. Isatin analogues bearing C5- and C6-benzyloxy substituents (**2** and **3**) were particularly potent reversible MAO-B inhibitors with  $IC_{50}$  values of 0.103 and 0.138  $\mu$ M, respectively.<sup>29</sup> The high binding affinities of the substituted isatin analogues to MAO-B may be explained by modeling studies which suggest that the isatin dioxindolyl ring is bound to the substrate cavity while the C5 and C6 substituents extend into the entrance cavity. The additional productive interactions of the C5 and C6 substituents with the entrance cavity amino acid residues may allow for higher binding affinities to the enzyme compared to isatin and hence more potent inhibition.<sup>28,29</sup> Isatin may therefore be considered as a promising scaffold for the design of MAO inhibitors. Based on these observations the present study examines a series of phthalimide analogues as potential inhibitors of MAO-A and -B. Phthalimide (**4**) is an isomer of isatin and appropriately substituted phthalimide analogues may therefore also possess affinity for the MAO isozymes (Fig. 2). To explore this possibility, 5-benzyloxyphthalimide (**5a**) and other selected 5-alkyloxy- and 5-aryloxyphthalimides (**5b–i**) were synthesized and evaluated as inhibitors of MAO-A and -B (Scheme 1). As discussed above, the benzyloxy side chain was selected as initial substituent in this study since it has been shown to enhance the binding affinity of isatin to particularly MAO-B.

## 2. Results and discussion

### 2.1. Chemistry

In the present study selected 5-alkyloxy- and 5-aryloxyphthalimides (**5a–i**) were synthesized with the aim of examining their



**Scheme 1.** The synthetic route to the 5-alkoxy- and 5-aryloxyphthalimides (**5a–i**) that were examined in this study. Reagents: (a) NaOC<sub>2</sub>H<sub>5</sub>; (b) HNO<sub>3</sub> (10%).

**Table 1**

<sup>1</sup>H NMR and <sup>13</sup>C NMR chemical shifts for the NH proton and carbonyl C1 and C3 of phthalimide analogues **5a–i**<sup>a</sup>

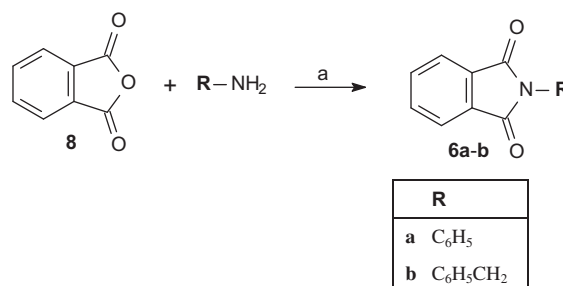
R	NH	C1/C3
<b>5a</b> C <sub>6</sub> H <sub>5</sub> O	11.26	168.4
<b>5b</b> C <sub>6</sub> H <sub>5</sub> CH <sub>2</sub> O	11.18	168.8
<b>5c</b> C <sub>6</sub> H <sub>5</sub> CH <sub>2</sub> CH <sub>2</sub> O	11.16	168.8
<b>5d</b> C <sub>6</sub> H <sub>5</sub> (CH <sub>2</sub> ) <sub>3</sub> O	11.63	168.8
<b>5e</b> (E)-C <sub>6</sub> H <sub>5</sub> CH=CHCH <sub>2</sub> O	11.18	168.8
<b>5f</b> 2-Naphthalenyl-O	11.32	168.4
<b>5g</b> 4-BrC <sub>6</sub> H <sub>4</sub> CH <sub>2</sub> O	11.19	168.8
<b>5h</b> 4-BrC <sub>6</sub> H <sub>4</sub> CH <sub>2</sub> CH <sub>2</sub> O	11.18	168.8
<b>5i</b> 4-BrC <sub>6</sub> H <sub>4</sub> O	11.33	168.4

<sup>a</sup> The NMR experiments were conducted in DMSO-*d*<sub>6</sub> (see Section 4).

MAO inhibitory properties. The target phthalimides were prepared from the corresponding C4-substituted phthalonitriles (**7a–i**) as shown in Scheme 1. The phthalonitriles were treated with a solution of sodium ethoxide followed by dilute nitric acid to yield the phthalimide analogues **5a–i** in poor to good yields (10–81%).<sup>30</sup> The successful formation of the phthalimide ring system of the target compounds were verified by the presence of two <sup>13</sup>C NMR signals at 168.4–168.9 ppm which corresponds to the carbonyl carbons at C1 and C3 and the presence of a <sup>1</sup>H NMR signal at approximately 11 ppm which corresponds to the phthalimide NH proton (Table 1). The C4-substituted phthalonitriles (**7a–i**) required for these synthesis were obtained by reacting 4-nitrophthalonitrile with the appropriate alcohol in the presence of potassium carbonate in dimethyl sulfoxide (DMSO) as described previously.<sup>31</sup> The N-substituted phthalimide analogues **6a–c** were, in turn, prepared by reacting phthalic anhydride (**8**) with the appropriate amine in glacial acetic acid (Scheme 2).<sup>32</sup> In each instance, the structures and purities of the target compounds were verified by <sup>1</sup>H NMR, <sup>13</sup>C NMR, mass spectrometry and HPLC analysis as cited in the experimental section.

## 2.2. MAO inhibition studies

To examine the 5-alkoxy- and 5-aryloxyphthalimide analogues **5a–i** as potential inhibitors of MAO-A and -B, microsomes from insect cells containing the recombinant human enzymes



**Scheme 2.** The synthetic route to the N-substituted phthalimide analogues **6a** and **6b**. Reagents: (a) glacial acetic acid.

were employed.<sup>29,33,34</sup> The MAO-A/B mixed substrate, kynuramine, was used to measure the catalytic rates of the enzymes in the absence and presence of various concentrations of the test inhibitors.<sup>33</sup> Kynuramine is oxidized by the MAO enzymes to yield the fluorescent metabolite, 4-hydroxyquinoline. Concentration measurements of 4-hydroxyquinoline were conveniently carried out by fluorescence spectrophotometry (excitation wavelength of 310; emission wavelength of 400 nm) since none of the inhibitors investigated in this study fluoresced at these excitation/emission wavelengths or quenched the fluorescence of 4-hydroxyquinoline at the inhibitor concentrations used.<sup>35</sup> The inhibition potencies of the test inhibitors were calculated from the experimentally obtained sigmoidal dose–response curves and expressed as the IC<sub>50</sub> values (Fig. 3). Using the Cheng-Prusoff equation,<sup>36,37</sup> the isoform selectivity index [SI = K<sub>i</sub>(MAO-A)/K<sub>i</sub>(MAO-B)] of each inhibitor was calculated. For this purpose the experimentally determined IC<sub>50</sub> values were converted to the corresponding K<sub>i</sub> values for the inhibition of MAO-A and MAO-B.

The recombinant human MAO inhibition data for the 5-alkoxy- and 5-aryloxyphthalimide analogues (**5a–i**) are presented in Table 2. For comparison, the reported MAO-A and -B inhibition potencies of isatin (**1**), 5-benzyloxyisatin (**2**) and 6-benzyloxyisatin (**3**) are also given.<sup>29</sup> Compared to isatin (**1**), 5-benzyloxyisatin (**2**) and 6-benzyloxyisatin (**3**), the phthalimides were in general superior MAO-B inhibitors with IC<sub>50</sub> values ranging from 0.007–2.49 μM. The only exception was **5a**, the phenoxy substituted phthalimide (IC<sub>50</sub> = 2.49 μM), which were a weaker MAO-B inhibitor than 5-benzyloxyisatin (IC<sub>50</sub> = 0.103 μM) and 6-benzyloxyisatin (IC<sub>50</sub> = 0.138 μM) but still approximately fivefold more potent than isatin (IC<sub>50</sub> = 12.4 μM). Increasing the length of the C5 substituent enhances the MAO-B inhibition potencies of the phthalimide analogues by several orders of a magnitude. For example, substitution at C5 with a benzyloxy moiety yields compound **5b** with an IC<sub>50</sub> value of 0.043 μM, approximately 58-fold more potent than the phenoxy substituted phthalimide **5a**. Similarly, substitution with the phenylethoxy (**5c**) and phenylpropoxy (**5d**) side chains also yielded exceptionally potent MAO-B inhibitors with IC<sub>50</sub> values of 0.017 μM and 0.050 μM, respectively. Even introduction of an ethenyl double bond into the phthalimide C5 side chain, as observed with the phenylpropenyl derivative **5e**, yielded a potent MAO-B inhibitor (IC<sub>50</sub> = 0.046 μM). Interestingly, replacing the phenyl ring of the C5 substituent of **5a** with a naphthalenyl ring yielded the exceptionally potent MAO-B inhibitor **5f** with an IC<sub>50</sub> value 0.033 μM. Compound **5f** is 75-fold more potent than **5a** as an MAO-B inhibitor. This result further demonstrates that increasing the length or size of the C5 substituent enhances the MAO-B inhibition potencies of the phthalimide analogues. This result also shows that the length or size of the substituent may be increased by increasing the length of the oxy linker between the phthalimide and phenyl rings or by modifying the phenyl ring to enhance its size, by for example replacement with a naphthalenyl ring. To

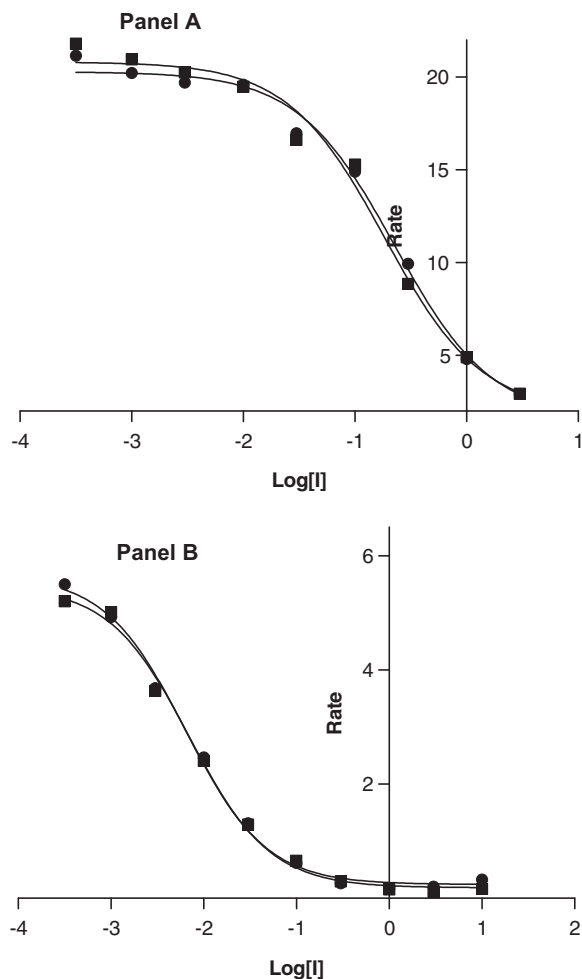


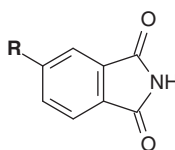
**Figure 3.** The sigmoidal dose–response curves of the initial rates of oxidation of kynuramine by recombinant human MAO-A (Panel A) and recombinant human MAO-B (Panel B) vs. the logarithm of concentration of inhibitor **5g** (expressed in μM). The determinations were carried out in duplicate and the values are expressed as the mean ± SD. The concentrations of kynuramine used were 45 and 30 μM for the studies with MAO-A and MAO-B, respectively, and the rate data are expressed as nmoles 4-hydroxyquinoline formed/min/mg protein.

examine the possibility of further enhancing the MAO-B inhibition potency of the C5 substituted phthalimide analogues discussed above, the phenyl rings of the C5 substituent of selected homologues (**5a–c**) were substituted with bromine. Bromine was selected since previous studies have shown that halogen substitution, and in particular bromine substitution, on the phenyl ring of the C8 substituent of benzyloxycaffeine<sup>34</sup> and styrylcaffeine<sup>38</sup> derivatives enhances the MAO-B inhibition potencies of these compounds by several orders of a magnitude. In accordance with this view, phthalimide analogue **5i**, the bromine substituted homologue of **5a** exhibited an  $IC_{50}$  value for the inhibition of MAO-B of 0.055 μM, 45-fold more potent than **5a** ( $IC_{50}$  = 2.49 μM). Phthalimide analogue **5g**, the bromine substituted homologue of **5b** was found to be the most potent MAO-B inhibitor of the present series with an  $IC_{50}$  value of 0.0069 μM, sixfold more potent than **5b** ( $IC_{50}$  = 0.043 μM). Noteworthy is the observation that compound **5c** ( $IC_{50}$  = 0.017 μM) is approximately fourfold more potent as an MAO-B inhibitor than its bromine substituted homologue, **5h** ( $IC_{50}$  = 0.067 μM). These results indicate that while halogen substitution on the phenyl ring of the C5 side chain enhances the MAO-B inhibition potencies of weaker phthalimide inhibitors (**5a**) to a large degree, its effects on the MAO-B inhibition potencies of the more potent phthalimide analogues (**5b**, **5c**) are less remarkable.

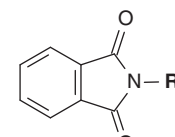
Halogen substitution on the ring system of the C5 side chain may therefore be viewed as a general strategy to enhance the MAO-B inhibition potency of moderate and weak phthalimide inhibitors.

The importance of the C5 substituent for MAO-B inhibition was demonstrated by the finding that phthalimide (**4**) is a weak MAO-B inhibitor with an  $IC_{50}$  value of 134 μM (Table 3). This is approximately 11-fold weaker than the MAO-B inhibition potency recorded for isatin ( $IC_{50}$  = 12.4 μM) and approximately 54-fold weaker than the inhibition potency recorded for **5a**, the weakest C5 substituted phthalimide analogue of the studied series ( $IC_{50}$  = 2.49 μM). Also, the significance of the positioning of the substituent at C5 of the phthalimide ring was demonstrated by the finding that the N-substituted isomers **6a** and **6b** only inhibits MAO-B at very high concentrations (Table 3). These results show that a C5 substituent is critical for the MAO-B inhibition activity of phthalimide and that the position of the substituent on the phthalimide ring system is also an important consideration. This behavior will be further explored below with the aid of molecular docking studies.

The 5-alkoxy- and 5-aryloxyphthalimide analogues **5a–i** were also evaluated as potential inhibitors of recombinant human MAO-A (Table 2). With the exception of **5a**, the phthalimide analogues displayed weaker MAO-A inhibition potencies compared to their corresponding MAO-B inhibition potencies. Based on the isoform SI values, these analogues (**5b–i**) were 10- to 129-fold more potent as MAO-B inhibitors. Compound **5a** was essentially a non-selective MAO-A/B inhibitor. The most potent MAO-A inhibitor among the test compounds was **5g**, the bromobenzyloxy substituted analogue, with an  $IC_{50}$  value of 0.22 μM. Similar to the trend observed for the inhibition of MAO-B, bromine substitution on the phenyl ring of the C5 substituent enhances the MAO-A inhibition potencies. For example, **5g** is approximately 19-fold more potent than its corresponding unsubstituted homologue **5b** ( $IC_{50}$  = 4.17 μM). Similarly, bromine substituted compounds **5h** ( $IC_{50}$  = 1.08 μM) and **5i** ( $IC_{50}$  = 1.08 μM) were also more potent than their corresponding unsubstituted homologues **5c** ( $IC_{50}$  = 3.58 μM) and **5a** ( $IC_{50}$  = 5.85 μM), respectively, although to lesser extents (3–5-fold) than observed for **5b**. Also similar to MAO-B, substitution of the phenyl ring of the C5 substituent of **5a** with a naphthalenyl ring significantly improved the MAO-A inhibition potency with inhibitor **5f** displaying an  $IC_{50}$  value of 0.92 μM, approximately sixfold more potent than **5a**. In fact, **5f** was the second most potent MAO-A inhibitor among the phthalimides evaluated. Increasing the C5 side chain length also enhanced the MAO-A inhibition potencies of the phthalimide analogues, although by a relatively small extent. For example the phenoxy (**5a**), benzyloxy (**5b**), phenylethoxy (**5c**) and phenylpropoxy (**5d**) substituted analogues exhibited  $IC_{50}$  values of 5.85, 4.17, 3.58 and 1.73 μM, respectively. Interestingly, the phenylpropenyloxy substituted analogue **5e** ( $IC_{50}$  = 8.99 μM) was found to be the weakest MAO-A inhibitor among the phthalimides. In a previous study it was found that a C8 substituent with a relatively large degree of flexibility is a requirement for caffeine analogues to act as MAO-A inhibitors. For example, 8-benzyloxycaffeine (**9**)<sup>34</sup> and some of its analogues are inhibitors of both MAO-A and -B, while (*E*)-8-styrylcaffeine (**10**)<sup>38,39</sup> is a MAO-B selective inhibitor with no observed affinity for MAO-A (Fig. 4). Modeling studies have suggested that the ability of the 8-benzyloxycaffeine analogues to bind to the MAO-A active site may, to a large degree, depend on the relatively large degree of rotational freedom of the benzyloxy side chain at the carbon-oxygen ether bond.<sup>34</sup> In contrast, the more conformationally rigid (*E*)-styryl side chain is less well accommodated by the MAO-A active site. A possible reason for the relatively weaker MAO-A inhibition potency of **5e** may therefore be that, due to the ethenyl double bond, its phenylpropenyloxy side chain is less flexible than that of the other phthalimides examined here, and

**Table 2**The IC<sub>50</sub> values and calculated K<sub>i</sub> values for the inhibition of recombinant human MAO-A and -B by phthalimide analogues **5a–i**<sup>a</sup>


	R	IC <sub>50</sub> (μM)		K <sub>i</sub> <sup>b</sup> (μM)		SI <sup>c</sup>
		MAO-A	MAO-B	MAO-A	MAO-B	
<b>5a</b>	C <sub>6</sub> H <sub>5</sub> O	5.85 ± 0.203	2.49 ± 0.0057	1.54	1.073	1
<b>5b</b>	C <sub>6</sub> H <sub>5</sub> CH <sub>2</sub> O	4.17 ± 2.082	0.043 ± 0.0081	1.1	0.019	59
<b>5c</b>	C <sub>6</sub> H <sub>5</sub> CH <sub>2</sub> CH <sub>2</sub> O	3.58 ± 0.461	0.017 ± 0.0026	0.94	0.007	129
<b>5d</b>	C <sub>6</sub> H <sub>5</sub> (CH <sub>2</sub> ) <sub>3</sub> O	1.73 ± 0.364	0.050 ± 0.0093	0.46	0.02	21
<b>5e</b>	( <i>E</i> )-C <sub>6</sub> H <sub>5</sub> CH=CHCH <sub>2</sub> O	8.99 ± 0.130	0.046 ± 0.0053	2.37	0.020	120
<b>5f</b>	2-Naphthalenyl-O	0.92 ± 0.024	0.033 ± 0.0040	0.2	0.01	17
<b>5g</b>	4-BrC <sub>6</sub> H <sub>4</sub> CH <sub>2</sub> O	0.22 ± 0.031	0.0069 ± 0.0003	0.058	0.003	20
<b>5h</b>	4-BrC <sub>6</sub> H <sub>4</sub> CH <sub>2</sub> CH <sub>2</sub> O	1.08 ± 0.160	0.067 ± 0.015	0.285	0.029	10
<b>5i</b>	4-BrC <sub>6</sub> H <sub>4</sub> O	1.08 ± 0.316	0.055 ± 0.017	0.285	0.024	12
<b>1</b>	Isatin <sup>d</sup>	31.8	12.4	8.38	5.34	1.6
<b>2</b>	5-Benzyloxyisatin <sup>d</sup>	4.62	0.103	1.22	0.044	27
<b>3</b>	6-Benzyloxyisatin <sup>d</sup>	72.4	0.138	19.1	0.059	321

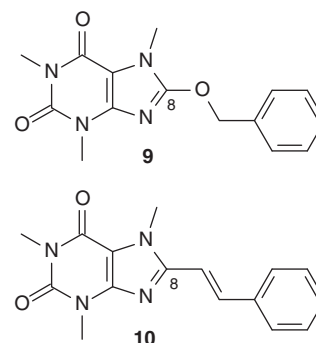
<sup>a</sup> All values are expressed as the mean ± SD of duplicate determinations.<sup>b</sup> The K<sub>i</sub> values were calculated from the experimentally measured IC<sub>50</sub> values according to the equation by Cheng and Prusoff: K<sub>i</sub> = IC<sub>50</sub>/(1 + [S]/K<sub>m</sub>) with [S] = 45 μM and K<sub>m</sub> (kynuramine) = 16.1 μM for human MAO-A and [S] = 30 μM and K<sub>m</sub> (kynuramine) = 22.7 μM for human MAO-B.<sup>34,36</sup><sup>c</sup> The selectivity index is the selectivity for the MAO-B isoform and is given as the ratio of K<sub>i</sub>(MAO-A)/K<sub>i</sub>(MAO-B).<sup>d</sup> Inhibition values for these compounds obtained from Ref. 29.**Table 3**The inhibition of recombinant human MAO-A and -B by phthalimide (**4**) and N-substituted phthalimide analogues (**6a** and **6b**)


	R	IC <sub>50</sub> <sup>a,b</sup> (μM) or %inhibition <sup>b,c</sup>	
		MAO-A	MAO-B
<b>4</b>	H	165 ± 12.5 <sup>a</sup>	134 ± 1.63 <sup>a</sup>
<b>6a</b>	C <sub>6</sub> H <sub>5</sub>	10.5 ± 3.64% <sup>c</sup>	50.3 ± 0.38% <sup>c</sup>
<b>6b</b>	C <sub>6</sub> H <sub>5</sub> CH <sub>2</sub>	No inhibition <sup>d</sup>	20.2 ± 5.09% <sup>c</sup>

<sup>a</sup> The IC<sub>50</sub> value is reported for this compound.<sup>b</sup> All values are expressed as the mean ± SD of duplicate determinations.<sup>c</sup> The %inhibition at a maximum tested concentration of 100 μM.<sup>d</sup> No inhibition observed at a maximum tested concentration of 100 μM.

therefore the least suited for binding to MAO-A. Possible explanations for this behavior will be explored in more detail below using molecular docking.

As observed for the MAO-B inhibition potencies, the C5 substituents of the phthalimides are important structural features for their observed MAO-A inhibition activities. This is illustrated by the finding that phthalimide (**4**) is a weak MAO-A inhibitor with an IC<sub>50</sub> value of 165 μM (Table 3). This is approximately 18-fold weaker than the MAO-A inhibition potency of the weakest C5 substituted phthalimide analogue of the studied series, compound **5e** (IC<sub>50</sub> = 8.99 μM). The significance of the positioning of the substituent at C5 of the phthalimide ring was also demonstrated for the inhibition of MAO-A by the finding that the N-substituted isomers were not MAO-A inhibitors (**6b**) or very weak inhibitors (**6a**), even at high concentrations (Table 3). Therefore, as for MAO-B inhibition, a substituent at C5 is a critical feature for the MAO-A inhibition activity of phthalimide.

**Figure 4.** The structures of 8-benzyloxycaffeine (**9**) and (*E*)-8-styrylcaffeine (**10**).

### 2.3. Reversibility studies

As discussed in the Introduction, from a therapeutic point of view, reversible inhibition of the MAO isoforms may have significant advantages over the inactivation of these enzymes. Isatin and C5- and C6-substituted isatin analogues have previously been shown to interact reversibly with human MAO-A and -B.<sup>28,29</sup> The phthalimide analogues that were investigated in this study were similarly evaluated for their ability to interact reversibly with MAO-A and -B. For this purpose the time dependence of the inhibition of human MAO-A and -B by one representative inhibitor, phthalimide **5a**, was evaluated. The concentrations of **5a** that were selected for these studies were 13.42 and 5.00 μM for the incubations with MAO-A and -B, respectively. These concentrations are approximately twofold the measured IC<sub>50</sub> values for the inhibition of the respective enzymes by **5a**. Compound **5a**, at these concentrations, and recombinant human MAO-A or -B were preincubated for periods of 0, 15, 30 and 60 min. Following the addition of the MAO-A/B mixed substrate, kynuramine, the residual catalytic activities of MAO-A and -B were measured.

The results of the time dependent studies are presented in Figure 5. As shown by the graphs, there are no time-dependent reductions in the catalytic rates of MAO-A and -B when phthalimide **5a** is preincubated with the enzyme preparations, even after a period of 60 min. These results lead to the conclusion that the inhibition of MAO-A and -B by **5a** is not time dependent and therefore reversible, at least for the time period (0–60 min) and at the inhibitor concentrations ( $2 \times \text{IC}_{50}$ ) evaluated. Interestingly, small but significant increases of the rates of the MAO-A and -B catalyzed oxidations of kynuramine with increased preincubation time of **5a** with the enzyme preparations are observed. A possible explanation for this behavior may be that phthalimide **5a** may slowly hydrolyze in the aqueous buffer (potassium phosphate 100 mM, pH 7.4) used in this study for the enzyme incubations. As a result, the concentration of the active phthalimide inhibitor may slowly decrease which results in a lesser degree of inhibition and therefore an increase in enzyme catalytic rate. This possibility is supported by literature reports that phthalimides undergo hydrolytic C–N bond fission to yield the ring-opened phthalamic acids.<sup>40</sup> In this study an incubation time of 20 min was selected for the determination of the inhibition potencies of the phthalimide analogues (Table 2). Considering that for **5a** only a small loss of inhibition potency is observed between the 15 min and 30 min time points, it may be concluded that relatively little hydrolysis has occurred at these

time points and that the effect of hydrolysis on the measured  $\text{IC}_{50}$  values should be small.

To provide further support for the finding that **5a** is a reversible inhibitor of both MAO-A and -B, the mode of enzyme inhibition was examined. For this purpose, sets of Lineweaver–Burk plots were constructed for the inhibition of MAO-A as well as MAO-B by inhibitor **5a**. The initial rates of the MAO-A or -B catalyzed oxidation of kynuramine at four different substrate concentrations (15–90  $\mu\text{M}$ ) were recorded in the absence and presence of various concentrations of inhibitor **5a**. For the studies with MAO-A the concentrations of inhibitor **5a** were 1.7–6.8  $\mu\text{M}$  while for the studies with MAO-B the concentrations of inhibitor **5a** were 0.625–2.5  $\mu\text{M}$ . The Lineweaver–Burk plots so obtained are presented in Figure 6. Inspection of these results reveals that for the inhibition of both MAO-A and -B by **5a**, the plots are linear and intersect at the y-axis. This suggests that the mode of inhibition is competitive and provide further support that **5a** interacts reversibly with the active sites of human MAO-A and -B.

## 2.4. Molecular modeling studies

The results of this study show that C5 substituted phthalimide analogues **5a–i** are inhibitors of recombinant human MAO-A and -B. An important observation was the critical importance of the C5 substituent for the MAO-A as well as MAO-B inhibition activities of the phthalimides. This was best demonstrated by the finding that phthalimide (**4**) and N-substituted phthalimides (**6a** and **6b**) are weak MAO-A and -B inhibitors and in some instances were found not to interact with the enzymes, even at high concentrations. Also of importance was the observation that the phenylpropenyloxy substituted analogue **5e** was the weakest MAO-A inhibitor among the phthalimides evaluated while exhibiting potent MAO-B inhibition activity. A possible explanation for this behavior may be that due to the presence of the ethenyl double bond, the phenylpropenyloxy side chain of **5e** is less flexible than that of the other C5 phthalimide side chains investigated, and therefore the least suited for binding to MAO-A. Literature suggests that at least for C8-substituted caffeines, a large degree of rotational freedom of the C8 side chain is a requirement for MAO-A inhibition.<sup>34</sup> To provide additional insight, the binding modes of selected phthalimides (**5e** and **6a**) in the active site cavities of MAO-A and -B were examined using molecular docking.

The molecular docking experiments were carried out with the Discovery Studio 1.7 modeling software according to a previously reported protocol.<sup>29,34</sup> As enzymatic models, the crystallographic structures of human MAO-A in complex with harmine (PDB entry: 2Z5X)<sup>41</sup> and human MAO-B in complex with safinamide (PDB entry: 2V5Z)<sup>42</sup> were selected. These models were selected based on the high resolution of the crystallographic structures and are frequently used in modeling studies.<sup>29,34</sup> The enzymatic models were prepared as described previously.<sup>29,34</sup> The valences of the FAD cofactor and the co-crystallized ligands (harmine and safinamide) were corrected, hydrogen atoms were added to the enzymatic models and the models were subjected to a three-step energy minimization cascade while the backbones of the enzymes were constrained. This was followed by the deletion of the co-crystallized ligands from the models and the detection of the binding cavities by the flood-filling algorithm. All crystal water molecules were removed from the enzymatic models except for those in the MAO-A and -B active sites that are considered conserved and non-displaceable (see Experimental). The structures of the phthalimide inhibitors (**5e** and **6a**) were constructed and their geometries optimized within Discovery Studio and were subsequently docked into the active sites of the MAO-A and -B models using the Ligand-Fit application within Discovery Studio. This protocol has been shown to be suitable for examining the binding of inhibitors to

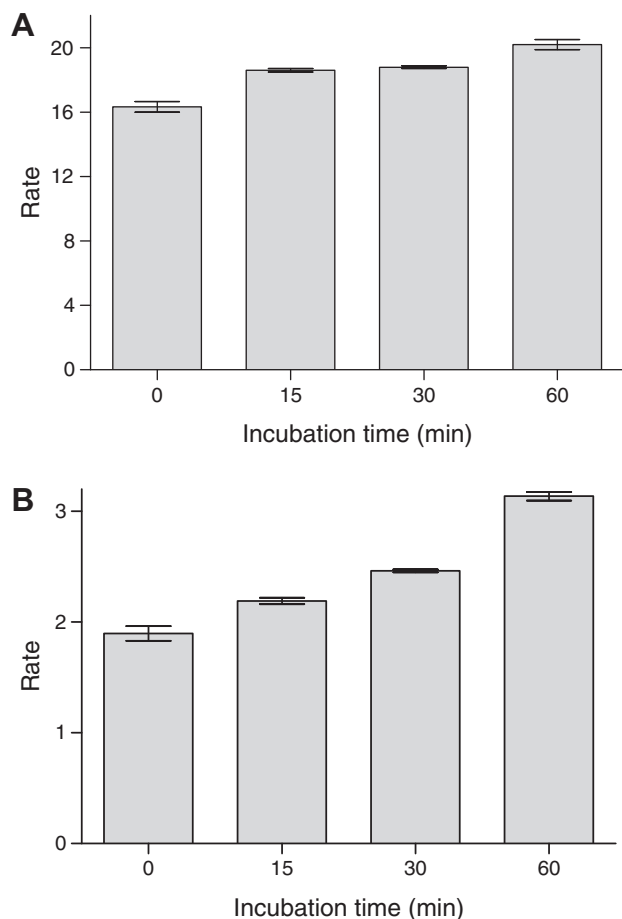


**Figure 5.** Time-dependant inhibition of recombinant human MAO-A (Panel A) and recombinant human MAO-B (Panel B) by phthalimide analogue **5a**. The enzymes were preincubated for various periods of time (0–60 min) with **5a** at concentrations of 13.42  $\mu\text{M}$  and 5.00  $\mu\text{M}$  for MAO-A and MAO-B, respectively. The concentrations of the enzyme substrate, kynuramine, were 45 and 30  $\mu\text{M}$  for the studies with MAO-A and MAO-B, respectively. The catalytic rates are expressed as nmoles 4-hydroxyquinoline formed/min/mg protein.

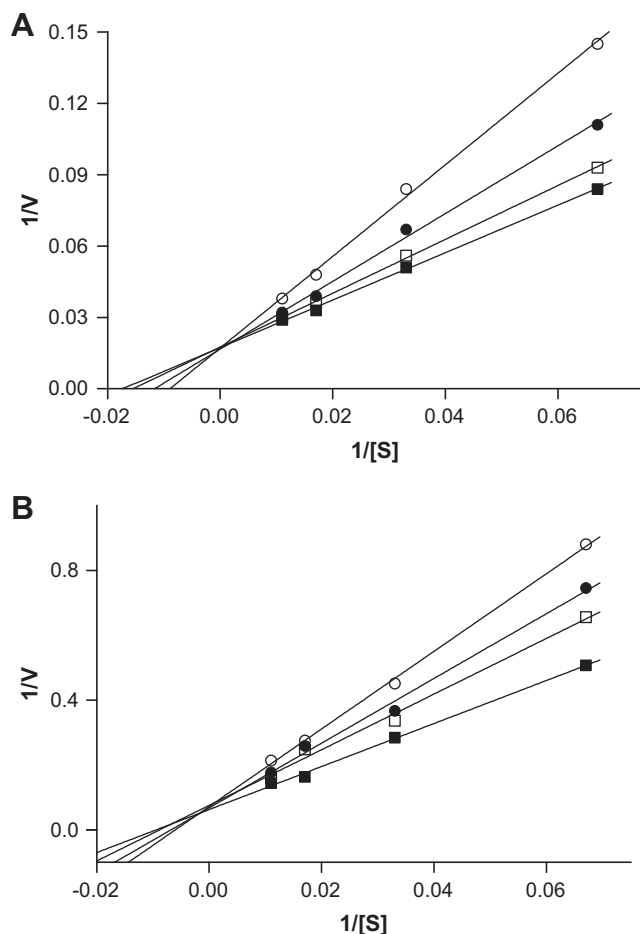


**Figure 6.** Lineweaver–Burk plots of the recombinant human MAO-A (Panel A) and recombinant human MAO-B (Panel B) catalyzed oxidation of kynuramine in the absence (filled squares) and presence of various concentrations of **5a**. For the studies with MAO-A (Panel A) the concentrations of **5a** were: 1.7  $\mu\text{M}$  (open squares), 3.4  $\mu\text{M}$  (filled circles), 6.8  $\mu\text{M}$  (open circles). For the studies with MAO-B (Panel B) the concentrations of **5a** were: 0.625  $\mu\text{M}$  (open squares), 1.25  $\mu\text{M}$  (filled circles), 2.5  $\mu\text{M}$  (open circles). The rates ( $V$ ) are expressed as nmol product formed/min/mg protein.

MAO-A and -B since redocking of harmine (RMSD = 0.64 Å) and safinamide (RMSD = 1.54 Å) into the active sites of the two enzymes, respectively, yielded binding orientations that exhibited relatively small RMSD values from the position of the co-crystallized ligands.<sup>29</sup>

The predicted binding orientation of compound **5e** within the active site model of MAO-B is displayed in Figure 7. In the MAO-B active site, the inhibitor adopts an orientation that positions the phthalimide ring within the substrate cavity of the enzyme while the C5 side chain extends towards the entrance cavity. This orientation is observed for all of the C5 substituted phthalimide analogues examined in this study (**5a–i**) (results shown for **5e** only). This binding mode places the phthalimide ring in close proximity to the flavin ring with the phthalimide NH proton located only 2.2 Å from N5 of the flavin. This region, the *re* side of the FAD cofactor, of the substrate cavity is considered polar and at least 4 potential hydrogen bond interactions may occur between the phthalimide ring of **5e** and the FAD cofactor and active site water molecules in this region. These include interactions between the carbonyl oxygen at C1 of the phthalimide ring and the integral water molecules HOH-1155 and HOH-1351. Potential hydrogen bond interactions may also occur between the phthalimide NH proton and the carbonyl oxygen at C4 of the FAD cofactor as well

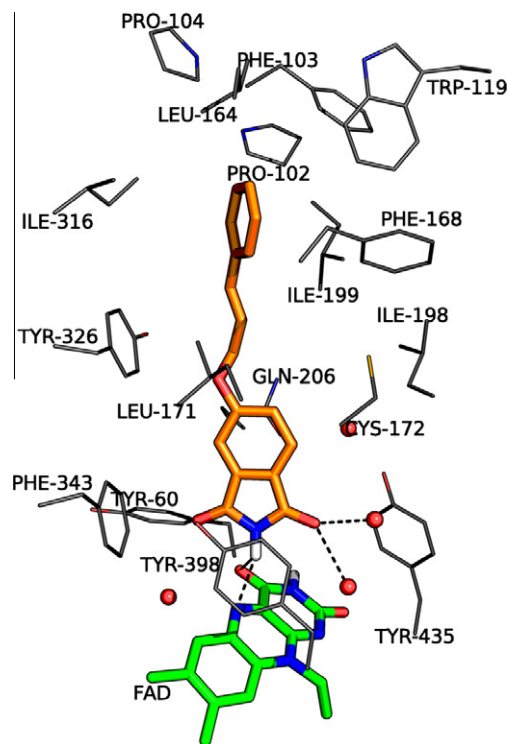


**Figure 7.** The predicted binding orientation of **5e** (orange colored) in the active site of MAO-B (2V5Z.pdb).

as with nitrogen N5 of the flavin. Also of significance is the observation that the phthalimide ring is orientated approximately parallel to the phenyl rings of the Tyr-398 and Tyr-435 side chains. This orientation is restricted by the flat shape of the substrate cavity of MAO-B<sup>43</sup> and places the plane of the phthalimide ring also approximately parallel to the plane of the amide functional group of the Gln-206 side chain. With an interplane distance of approximately 3.6 Å, a possible  $\pi$ – $\pi$  interaction between these two functional groups may be possible.<sup>41</sup> Also of importance is the observation that the phthalimide imidic N binds in the space where the amino groups of MAO-B substrates are thought to bind,<sup>44</sup> 3.3 Å from the C4a of the FAD cofactor. Modeling studies have suggested that the amine N of the MAO-B selective substrate, benzylamine, binds 3.7 Å from the C4a of the flavin.<sup>44</sup> As mentioned above, the C5 side chain of **5e** extends beyond the boundary of the substrate cavity, which is defined by the side chain of Ile-199, into entrance cavity of the MAO-B active site. Within the hydrophobic environment of the entrance cavity, the phenyl ring of the C5 side chain is most likely stabilized by Van der Waals interactions.<sup>45</sup> This binding orientation is similar to that observed for the co-crystallized inhibitor, safinamide, which also traverses both active site cavities.<sup>42</sup> Other relatively large inhibitors such as *trans,trans*-farnesol<sup>26</sup> and 1,4-diphenyl-2-butene<sup>27</sup> are also reported to span both the substrate and entrance cavities of the MAO-B active site. For these orientations to be possible, the side chain of Ile-199 should be rotated out of the normal conformation to allow for the fusion of the two cavities.<sup>26</sup> The importance of the interactions between the C5 side chain and the entrance cavity for stabilization of the phthalimide inhibitors may be demonstrated by the observation that phthalimide (**4**) is a very weak MAO-B inhibitor. Being a relatively small molecule compared to the C5 substituted derivatives, phthalimide is expected to bind only to the substrate cavity, leaving the entrance cavity unoccupied. As a result, phthalimide does not undergo stabilizing interactions with the entrance cavity and is therefore a weak MAO-B inhibitor. The interaction of the C5 side chain of the

phthalimide derivatives (**5a–i**) with the entrance cavity may also serve to position the phthalimide ring for optimal interaction with the polar region, the space in close proximity to the flavin. This view is supported by the observation that even though phthalimide (**4**) may interact with the polar region of the substrate cavity to a similar extent compared to the C5 substituted derivatives, it still possesses weak MAO-B inhibition activity. Further support for the view that a dual mode of binding to both the substrate and entrance cavities of MAO-B is crucial for the potent MAO-B inhibition activity of the phthalimide derivatives may be obtained by examining the predicted binding orientation of the N-substituted phthalimide, **6a**, in the MAO-B active site model. As shown in Figure 8, compound **6a** is orientated, similar to **5e**, with the phthalimide ring directed towards the FAD cofactor while the N-substituent extends towards the entrance cavity of the enzyme. In contrast to the orientation observed for **5e**, the phthalimide ring of **6a** is located relatively distant from the polar region of the substrate cavity, 4.4 Å from N5 of the flavin. As a result, no potential polar interactions between the phthalimide ring of **6a** and the polar functional groups of the substrate cavity of MAO-B are observed. The lack of stabilizing polar interactions between **6a** and the substrate cavity may explain the weak MAO-B inhibition activity of **6a**.

To examine possible reasons for the finding that the phthalimide derivatives are in general MAO-B selective inhibitors, potential binding orientations of compound **5e** within the MAO-A model was also calculated. As shown in Figure 9, the phthalimide ring of **5e** is orientated towards the FAD cofactor of MAO-A with the C5 side chain positioned in the region leading to the entrance of the active site. In contrast to its predicted orientation in MAO-B, **5e** binds more distant from the FAD cofactor, 3.2 Å from N5 of the flavin. In spite of this, compound **5e** is within hydrogen bond contact distance to several polar functional groups of the MAO-A active site. The carbonyl oxygen at C1 of the phthalimide ring may form hydrogen bonds with an active site water molecule (HOH-710)

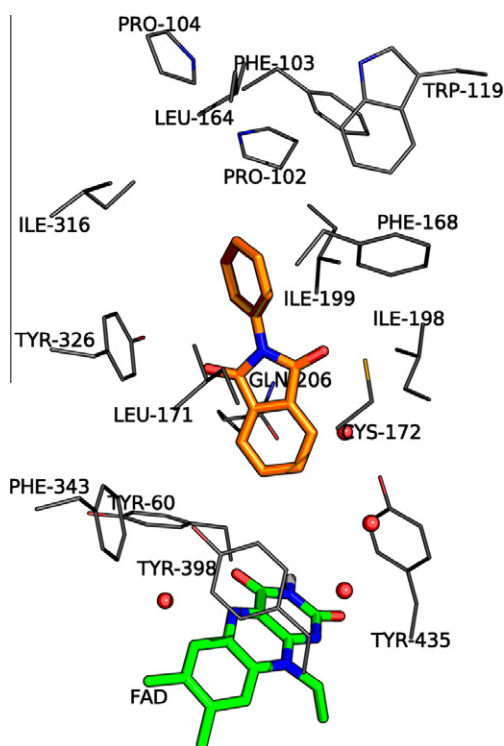


**Figure 8.** The predicted binding orientation of **6a** (orange colored) in the active site of MAO-B (2V5Z.pdb).

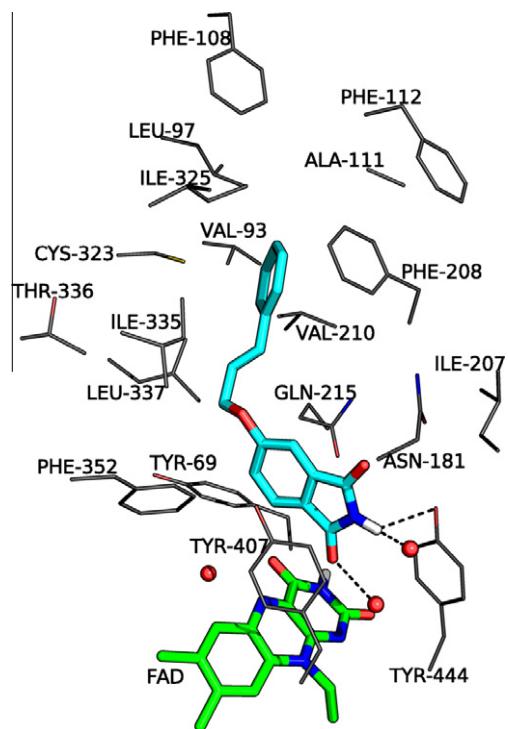


**Figure 9.** The predicted binding orientation of **5e** (cyan colored) in the active site of MAO-A (2Z5X.pdb).

while the phthalimide NH proton may form possible hydrogen bonds with the phenolic hydrogen of Tyr-444 and a water molecule (HOH-739). A possible  $\pi$ – $\pi$  interaction between the phthalimide ring and the amide functional group of the Gln-215 with an interplane distance of approximately 3.4 Å may also occur. Interestingly, **5e** is bound in a bent conformation with the C5 side chain bent by about a 50° angle from the plane of the caffeinyl ring (Fig. 10). Compound **5e** exists in this conformation in the MAO-A active site in order to avoid unfavorable interactions with the side chain of Phe-208. In the MAO-B active site, the residue corresponding to Phe-208 in MAO-A, is Ile-199. The increased size of the Phe aromatic ring compared to the side chain of Ile prevents the side chain of **5e** from occupying an extended conformation and the binding mode of **5e** observed in MAO-B would not be possible in the MAO-A active site.<sup>26,41</sup> As shown in Figure 11, if **5e** were to adopt the same orientation that is observed when it is bound to MAO-B, the C5 side chain would partially overlap with Phe-208 in the MAO-A active site. The relatively lower degree of flexibility of the phenylpropenyloxy side chain of **5e** may make it less ame-

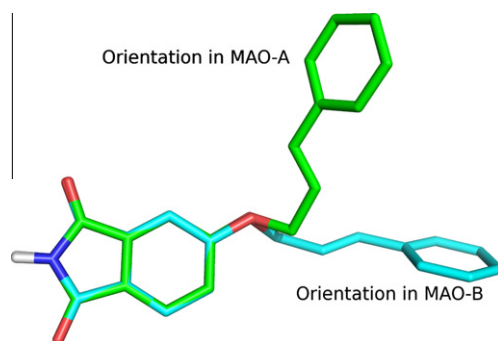


**Figure 10.** The docked orientations of **5e** within the active site of MAO-B (cyan colored) and MAO-A (green) with the phthalimide rings of the two respective orientations superimposed.

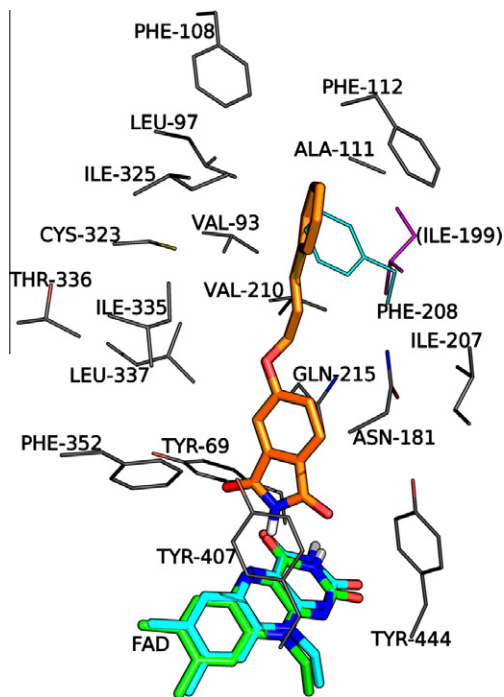


**Figure 11.** Illustration of the overlaid active sites of human MAO-A and -B. The binding orientation of compound **5e** (orange colored) as docked within the active site of MAO-B is shown here in the MAO-A active site. The active site residues of MAO-A are displayed in gray. Residue Ile-199 in MAO-B is displayed in magenta while residue Phe-208 in MAO-A is displayed in cyan.

nable for adopting orientations that avoid unfavorable interactions with the MAO-A active site residues. This may explain its lower binding affinity to MAO-A. Although **5e** is predicted to undergo several polar interactions with the active site of MAO-A, the results of the inhibition studies shows that it is approximately 120-fold more potent as an MAO-B inhibitor than an MAO-A inhibitor. This suggests that inhibitors that bind in close proximity to the FAD cofactor of MAO-A and -B would exhibit improved binding affinities compared to inhibitors that bind more distant.

### 3. Conclusion

In the present study, a series of C5 substituted phthalimide analogues **5a–i** were synthesized and evaluated as inhibitors of recombinant human MAO-A and -B. The results demonstrate that the analogues are exceptionally potent reversible MAO-B inhibitors with most analogues exhibiting  $IC_{50}$  values in the lower nM range. Analysis of the structure-activity relationships (SAR) reveals that increasing the length or size of the C5 substituent enhances the MAO-B inhibition potencies of the phthalimide analogues. Halogen substitution on the ring system of the C5 side chain also enhances MAO-B inhibition potency, particularly of the weaker phthalimide inhibitors. Importantly, the position of the substituent at C5 is an important structural feature since N-substituted phthalimides (**6a** and **6b**) are weak MAO-B inhibitors. Further evidence for the importance of the C5 substituent for binding to MAO-B is provided by the finding that phthalimide (**4**) is a weak MAO-B inhibitor. Modeling studies suggest that both polar interactions between the phthalimide ring and the polar region of the MAO-B substrate cavity and Van der Waals interactions between the C5 side chain and the entrance cavity are required for high affinity binding.<sup>45</sup> The view that interactions between the C5 side chain and the entrance cavity are important for inhibitor binding is supported by the finding that an enhancement of MAO-B inhibition activity is

observed with increasing length or size of the C5 substituent and halogen substitution on the aromatic ring of the C5 side chain. Both these structural modifications are expected to lead to more productive Van der Waals interactions between the C5 side chain and the entrance cavity. Since the phenyl ring of the C5 side chain is most likely stabilized to a large degree by Van der Waals interactions within the entrance cavity, halogen substitution on the phenyl ring (**5g–i**) is expected to enhance the productive interactions of the inhibitor with the entrance cavity of MAO-B via hydrophobic burial and dipole interactions. The enhancement of MAO-B inhibition potencies by halogen substitution has been previously reported.<sup>34</sup> For example, chlorine and bromine substitution on the benzyloxy phenyl ring of a series of 8-benzyloxycaffeines enhances the MAO-B inhibition potencies 20- and 22-fold, respectively.<sup>34</sup> Modeling studies suggest that this effect of halogen substitution is also dependent on the enhancement of productive hydrophobic and dipole interactions between the benzyloxy side chain and the MAO-B entrance cavity.<sup>34</sup>

The C5 substituted phthalimide analogues **5a–i** were also reversible inhibitors of MAO-A. With the exception of **5a** which is non-selective, the phthalimide analogues are however MAO-B selective inhibitors. Interestingly, similar to the results obtained with MAO-B, increasing the C5 side chain length and substitution with halogens on the aromatic ring of the C5 side chain also enhanced the MAO-A inhibition activities of the phthalimide analogues, although to a lesser extent as observed for MAO-B. These results suggest that the C5 side chain undergoes significant productive interactions with the MAO-A active site. The importance of the C5 side chain for binding to MAO-A was further demonstrated by the finding that phthalimide (**4**) is a weak MAO-A inhibitor. The findings that the N-substituted phthalimides are not MAO-A inhibitors (**6b**) or very weak inhibitors (**6a**) demonstrate that, as for MAO-B, the position of the side chain is an important consideration. Based on the analysis of possible binding modes of **5e** within the MAO-A active site it is proposed that relatively rigid C5 side chains are less suitable for adopting orientations that avoid unfavorable interactions with the MAO-A active site residues and inhibitors containing such side chains are therefore expected to possess lower affinities for MAO-A. Modeling studies suggests that although several polar interactions are possible between the phthalimide ring of the C5 substituted phthalimide analogues and the active site of MAO-A, the phthalimide analogues, do not bind in close proximity to the FAD cofactor. Since the phthalimide rings of these inhibitors are positioned very close to the flavin when binding in MAO-B, these results suggest that inhibitor binding in close proximity to the FAD cofactor is more favorable than binding more distant. These differing binding positions adopted by the inhibitors in MAO-A and -B may explain the observed higher binding affinities for the MAO-B active site.

In conclusion, C5 substituted phthalimides exhibit high binding affinities for MAO-B and are therefore promising lead compounds for the design of novel selective reversible inhibitors of MAO-B. In addition, certain analogues such as **5g**, which also possesses potent MAO-A inhibition activities, may act as lead compounds for the design of non-selective reversible MAO-A/B inhibitors.

## 4. Experimental section

### 4.1. Chemicals and instrumentation

Unless differently stated, all reagents and starting materials were obtained from Sigma–Aldrich and were used without further purification. Proton ( $^1H$ ) and carbon ( $^{13}C$ ) NMR spectra were recorded in DMSO-*d*<sub>6</sub> with a Bruker Avance III 600 spectrometer at frequencies of 600 MHz and 150 MHz, respectively. The NMR

chemical shifts are reported in parts per million ( $\delta$ ) downfield from the signal of tetramethylsilane added to the deuterated solvent and spin multiplicities are given as s (singlet), d (doublet), dd (doublet of doublets), t (triplet) or m (multiplet). Mass spectra (MS) and high resolution mass spectra (HRMS) were obtained on a DFS high resolution magnetic sector mass spectrometer (Thermo Electron Corporation) in atmospheric pressure chemical ionization (APCI) mode. Melting points (mp) were determined on a Stuart SMP10 melting point apparatus and are uncorrected. The degrees of purity of the target compounds were estimated by HPLC analyses using an Agilent 1200 HPLC system equipped with a quaternary pump and an Agilent 1200 series diode array detector (see [Supplementary data](#)). HPLC grade acetonitrile (Merck) and Milli-Q water (Millipore) were used for the chromatography. A Varian Cary Eclipse fluorescence spectrophotometer was used for all fluorescence measurements. Kynuramine-2HBr, 4-hydroxyquinoline and microsomes from insect cells containing recombinant human MAO-A and -B (5 mg/mL) were obtained from Sigma-Aldrich.

## 4.2. Synthesis of C5-substituted phthalimide analogues (5a–i)

The C5-substituted phthalimide analogues (**5a–i**) investigated in this study were synthesized according to the literature description.<sup>30</sup> The appropriate C4-substituted phthalonitrile analogue (**7a–i**) (7 mmol) was added at 15 °C to a solution of sodium ethoxide (prepared from 0.25 g sodium and 15 mL ethanol). The reaction mixture was stirred at 15 °C for a period of 2 h and poured into 25 mL nitric acid (10%). The mixture was stirred for 30 min and the resulting precipitate was collected by filtration, washed with 150 mL water and dried. The material was purified by at least two successive rounds of recrystallization from ethanol.

### 4.2.1. 5-Phenoxyphthalimide (5a)

The title compound was prepared from 4-phenoxyphthalonitrile (**7a**) in a yield of 24%: mp 171–173 °C (ethanol). <sup>1</sup>H NMR (600 MHz, DMSO-*d*<sub>6</sub>)  $\delta$  7.18 (m, 3H), 7.29 (t, 1H, *J* = 7.53 Hz), 7.33 (dd, 1H, *J* = 2.3, 8.3 Hz), 7.49 (t, 2H, *J* = 7.9 Hz), 7.81 (d, 1H, *J* = 7.91 Hz), 11.26 (s, 1H); <sup>13</sup>C NMR (600 MHz, DMSO-*d*<sub>6</sub>)  $\delta$  111.0, 120.3, 122.6, 125.3, 126.5, 130.6, 135.3, 154.7, 162.6, 168.4, 168.6; APCI-MS 239; APCI-HRMS *m/z*: calcd 239.0582, found 239.0580; Purity (HPLC): 99.6%.

### 4.2.2. 5-Benzyloxyphthalimide (5b)

The title compound was prepared from 4-benzyloxyphthalonitrile (**7b**) in a yield of 84%: mp 159–161 °C (ethanol). <sup>1</sup>H NMR (600 MHz, DMSO-*d*<sub>6</sub>)  $\delta$  5.28 (s, 2H), 7.36 (m, 2H), 7.40 (m, 3H), 7.47 (d, 2H, *J* = 7.5 Hz), 7.74 (d, 1H, *J* = 8.3 Hz), 11.18 (s, 1H); <sup>13</sup>C NMR (600 MHz, DMSO-*d*<sub>6</sub>)  $\delta$  70.1, 108.6, 120.7, 124.6, 124.8, 127.8, 128.1, 128.5, 135.2, 136.1, 163.3, 168.8, 168.9; APCI-MS 253; APCI-HRMS *m/z*: calcd 253.0739, found 253.0743; Purity (HPLC): 99.8%.

### 4.2.3. 5-(2-Phenylethoxy)phthalimide (5c)

The title compound was prepared from 4-(2-phenylethoxy)phthalonitrile (**7c**) in a yield of 10%: mp 167–169 °C (ethanol). <sup>1</sup>H NMR (600 MHz, DMSO-*d*<sub>6</sub>)  $\delta$  3.06 (t, 2H, *J* = 6.8 Hz), 4.36 (t, 2H, *J* = 6.8 Hz), 7.21 (t, 1H, *J* = 7.2 Hz), 7.31 (m, 6H), 7.70 (d, 1H, *J* = 8.3 Hz), 11.16 (s, 1H); <sup>13</sup>C NMR (600 MHz, DMSO-*d*<sub>6</sub>)  $\delta$  34.6, 69.1, 108.4, 120.3, 124.5, 124.8, 126.4, 128.4, 129.0, 135.3, 138.0, 163.5, 168.8, 168.9; APCI-MS 267; APCI-HRMS *m/z*: calcd 267.0895, found 267.0891; Purity (HPLC): 99.9%.

### 4.2.4. 5-(3-Phenylpropoxy)phthalimide (5d)

The title compound was prepared from 4-(3-phenylpropoxy)phthalonitrile (**7d**) in a yield of 15%: mp 147–149 °C (ethanol). <sup>1</sup>H NMR (600 MHz, DMSO-*d*<sub>6</sub>)  $\delta$  2.50 (m, 2H), 3.20 (t, 2H,

*J* = 7.9 Hz), 4.58 (t, 2H, *J* = 6.0 Hz), 7.64 (t, 1H, *J* = 7.2 Hz), 7.68 (d, 2H, *J* = 7.5 Hz), 7.74 (m, 4H), 8.17 (d, 1H, *J* = 9.0 Hz), 11.63 (s, 1H); <sup>13</sup>C NMR (600 MHz, DMSO-*d*<sub>6</sub>)  $\delta$  30.1, 31.4, 67.9, 108.3, 120.3, 124.4, 124.8, 125.9, 128.3, 128.4, 135.3, 141.2, 163.7, 168.8, 168.9; APCI-MS 281; APCI-HRMS *m/z*: calcd 281.1052, found 281.1041; Purity (HPLC): 97.4%.

### 4.2.5. 5-[(2E)-3-Phenylprop-2-en-1-yl]oxyphthalimide (5e)

The title compound was prepared from 4-[(2E)-3-phenylprop-2-en-1-yl]oxyphthalonitrile (**7e**) in a yield of 45%: mp 181–183 °C (ethanol). <sup>1</sup>H NMR (600 MHz, DMSO-*d*<sub>6</sub>)  $\delta$  4.88 (d, 2H, *J* = 5.7 Hz), 6.50 (m, 1H), 6.78 (d, 1H, *J* = 15.8 Hz), 7.26 (t, 1H, *J* = 7.2 Hz), 7.32 (m, 4H), 7.47 (d, 2H, *J* = 7.2 Hz), 7.72 (d, 1H, *J* = 7.9 Hz), 11.18 (s, 1H); <sup>13</sup>C NMR (600 MHz, DMSO-*d*<sub>6</sub>)  $\delta$  69.0, 108.6, 120.5, 124.0, 124.6, 124.8, 126.5, 128.1, 128.7, 133.1, 135.2, 136.0, 163.3, 168.8, 168.9; APCI-MS 279; APCI-HRMS *m/z*: calcd 279.0895, found 279.0883; Purity (HPLC): 97.4%.

### 4.2.6. 5-(Naphthalen-2-yloxy)phthalimide (5f)

The title compound was prepared from 4-(naphthalen-2-yloxy)phthalonitrile (**7f**) in a yield of 42%: mp 205–209 °C (ethanol). <sup>1</sup>H NMR (600 MHz, DMSO-*d*<sub>6</sub>)  $\delta$  7.28 (d, 1H, *J* = 1.9 Hz), 7.37 (dd, 1H, *J* = 2.3, 9.0 Hz), 7.41 (dd, 1H, *J* = 2.3, 8.3 Hz), 7.53 (m, 2H), 7.65 (d, 1H, *J* = 2.3 Hz), 7.83 (d, 1H, *J* = 7.9 Hz), 7.89 (d, 1H, *J* = 7.9 Hz), 7.97 (d, 1H, *J* = 7.9 Hz), 8.05 (d, 1H, *J* = 9.0 Hz), 11.32 (s, 1H); <sup>13</sup>C NMR (600 MHz, DMSO-*d*<sub>6</sub>)  $\delta$  111.5, 116.2, 120.2, 122.9, 125.4, 125.7, 126.7, 127.0, 127.4, 127.8, 130.6, 130.7, 133.9, 135.3, 152.5, 162.5, 168.4, 168.6; APCI-MS 289; APCI-HRMS *m/z*: calcd 289.0739, found 289.0730; Purity (HPLC): 99.6%.

### 4.2.7. 5-(4-Bromobenzyloxy)phthalimide (5g)

The title compound was prepared from 4-(4-bromobenzyloxy)phthalonitrile (**7g**) in a yield of 60%: mp 249–251 °C (ethanol). <sup>1</sup>H NMR (600 MHz, DMSO-*d*<sub>6</sub>)  $\delta$  5.26 (s, 2H), 7.35 (d, 1H, *J* = 8.7 Hz), 7.38 (s, 1H), 7.43 (d, 2H, *J* = 7.9 Hz), 7.59 (d, 2H, *J* = 7.9 Hz), 7.73 (d, 1H, *J* = 8.3 Hz), 11.19 (s, 1H); <sup>13</sup>C NMR (600 MHz, DMSO-*d*<sub>6</sub>)  $\delta$  69.3, 108.6, 120.7, 121.3, 124.8, 130.0, 131.5, 135.2, 135.6, 163.1, 168.8, 168.9; APCI-MS 330; APCI-HRMS *m/z*: calcd 330.9844, found 330.9897; Purity (HPLC): 98.6%.

### 4.2.8. 5-[2-(4-Bromophenyl)ethoxy]phthalimide (5h)

The title compound was prepared from 4-[2-(4-bromophenyl)ethoxy]phthalonitrile (**7h**) in a yield of 81%: mp 220 °C (ethanol). <sup>1</sup>H NMR (600 MHz, DMSO-*d*<sub>6</sub>)  $\delta$  3.05 (t, 2H, *J* = 6.4 Hz), 4.36 (t, 2H, *J* = 6.4 Hz), 7.27 (d, 1H, *J* = 8.3 Hz), 7.30 (m, 3H), 7.49 (d, 2H, *J* = 7.5 Hz), 7.71 (d, 1H, 8.3 Hz), 11.18 (s, 1H); <sup>13</sup>C NMR (600 MHz, DMSO-*d*<sub>6</sub>)  $\delta$  34.0, 68.8, 108.4, 119.6, 120.3, 124.5, 124.8, 131.2, 131.3, 135.3, 137.6, 163.4, 168.8, 168.9; APCI-MS 345, 347; APCI-HRMS *m/z*: calcd 345.0001, found 345.0001; Purity (HPLC): 97.2%.

### 4.2.9. 5-(4-Bromophenoxy)phthalimide (5i)

The title compound was prepared from 4-(4-bromophenoxy)phthalonitrile (**7i**) in a yield of 48%: mp 204–206 °C (ethanol). <sup>1</sup>H NMR (600 MHz, DMSO-*d*<sub>6</sub>)  $\delta$  7.14 (d, 2H, *J* = 8.7 Hz), 7.26 (d, 1H, *J* = 1.9 Hz), 7.36 (dd, 1H, *J* = 2.3, 8.3 Hz), 7.65 (d, 2H, *J* = 8.7 Hz), 7.82 (d, 1H, *J* = 8.3 Hz), 11.33 (s, 1H); <sup>13</sup>C NMR (600 MHz, DMSO-*d*<sub>6</sub>)  $\delta$  111.6, 117.1, 122.3, 123.0, 125.4, 127.0, 133.3, 135.3, 154.3, 161.9, 168.4, 168.6; APCI-MS 317, 319; APCI-HRMS *m/z*: calcd 316.9688, found 316.9685; Purity (HPLC): 99.8%.

## 4.3. Synthesis of N-substituted phthalimide analogues (6a and 6b)

The N-substituted phthalimide analogues (**6a** and **6b**) investigated in this study were synthesized according to the published

procedure.<sup>32</sup> A mixture of the appropriate amine (12 mmol) and phthalic anhydride (**8**; 10 mmol) were heated under reflux in 1 M acetic acid (20 mL) for 5 h. The reaction was allowed to cool to room temperature, water (100 mL) was added and the precipitated product was collected by filtration. The target N-substituted phthalimide analogues were recrystallized from 95% ethanol. The recorded melting points of **6a** and **6b** were 207–209 °C and 215–217 °C, respectively, while the reported melting points are 209–211 °C<sup>32</sup> and 215 °C,<sup>46</sup> respectively.

#### 4.4. The determination of IC<sub>50</sub> values for the inhibition of human MAO-A and -B

Microsomes (5 mg/mL) from baculovirus infected insect cells expressing recombinant human MAO-A or -B were obtained from Sigma-Aldrich and were pre-aliquoted (33 µL) and stored at –70 °C. All enzymatic reactions were carried out in potassium phosphate buffer (100 mM, pH 7.4, made isotonic with KCl, 20.2 mM) in microcentrifuge tubes (2 mL). The volumes of the reactions were 500 µL and the concentrations of MAO-A or MAO-B in the reactions were 0.0075 mg/mL. The stock solutions of the test inhibitors were prepared in DMSO and were added to the reactions to yield concentrations of the inhibitors of 0–100 µM and a concentration of 4% (v/v) DMSO. The MAO-A/B mixed substrate, kynuramine, was added to the reactions to yield final concentrations of 45 and 30 µM where MAO-A and -B, respectively, were used as enzymes. The reactions were incubated at 37 °C in a water bath for a period of 20 min and subsequently terminated with the addition of 400 µL NaOH (2 N). A volume of 1000 µL distilled water was added to each reaction, and the concentrations of the MAO generated 4-hydroxyquinoline in the reactions were measured by fluorescence spectrophotometry (excitation wavelength 310 nm, emission wavelength 400 nm).<sup>33</sup> Quantification of 4-hydroxyquinoline was achieved with a linear calibration curve constructed from solutions of authentic 4-hydroxyquinoline (0.047–1.5 µM) dissolved in 500 µL potassium phosphate buffer (100 mM, pH 7.4, made isotonic with KCl, 20.2 mM). Each calibration standard also contained 400 µL NaOH (2 N) and 1000 µL distilled water. Sigmoidal dose–response curves were constructed by plotting the initial rates of MAO catalyzed kynuramine oxidation versus the logarithm of the inhibitor concentration. Each curve, was constructed from 9 to 10 inhibitor concentrations spanning at least 3 orders of a magnitude. The inhibition data were fitted to the one site competition model incorporated into the Prism 5 software package (GraphPad). All experiments were carried out in duplicate and the IC<sub>50</sub> values are expressed as mean ± standard deviation (SD).<sup>34</sup> The IC<sub>50</sub> values were converted to the corresponding K<sub>i</sub> values according to the equation by Cheng and Prusoff:  $K_i = IC_{50} / (1 + [S]/K_m)$ .<sup>36</sup>

#### 4.5. Time-dependence of inhibition

For the purpose of the time dependent studies compound **5a** was selected as a representative inhibitor of the series. Compound **5a** and recombinant human MAO-A or human MAO-B (0.03 mg/mL) were preincubated for periods of 0, 15, 30, 60 min at 37 °C in potassium phosphate buffer (100 mM, pH 7.4, made isotonic with KCl, 20.2 mM). The concentrations of **5a** employed for these reactions were 13.42 µM and 5.00 µM for the incubations with MAO-A and -B, respectively. These are approximately twofold the measured IC<sub>50</sub> values for the inhibition of MAO-A and -B, respectively. To the preincubated enzyme preparations were then added the MAO-A/B mixed substrate, kynuramine, at final concentrations of 45 µM and 30 µM for the reactions containing MAO-A and -B, respectively. The volumes of these incubations were 500 µL, the final concentrations of the MAO preparations were 0.015 mg/mL and

the final concentrations of **5a** were 6.71 µM and 2.5 µM for MAO-A and MAO-B, respectively. These concentrations of **5a** are approximately equal to the IC<sub>50</sub> values for the inhibition of the respective enzyme preparations. The reactions were incubated for a further 15 min at 37 °C and subsequently terminated with 400 µL NaOH (2 N). A volume of 1000 µL distilled water was added to each reaction and the rates of the MAO-catalyzed production of 4-hydroxyquinoline were measured as described above. All measurements were carried out in triplicate and are expressed as mean ± SD.<sup>29,34</sup>

#### 4.6. Construction of Lineweaver–Burk plots

To evaluate the mode of MAO-A and -B inhibition, sets of Lineweaver–Burk plots for the inhibition of these enzymes by compound **5a** were constructed. By employing four different concentrations of the substrate, kynuramine (15, 30, 60 and 90 µM), the initial catalytic rates of the recombinant human enzymes were measured in the absence and presence of three different concentrations of **5a**. For the studies with MAO-A the concentrations of **5a** were 1.7, 3.4 and 6.8 µM. For the studies with MAO-B the concentrations of **5a** were 0.625, 1.25 and 2.5 µM. The enzymatic reactions and measurements were carried out as described above for the determination of the IC<sub>50</sub> values with the only exception that the concentrations of MAO-A and -B in the reactions were 0.015 mg/mL. Linear regression analysis was performed using the Prism 5 software package.<sup>34</sup>

#### 4.7. Molecular modeling studies

The Windows based Discovery Studio 1.7 molecular modeling software (Accelrys) was used for the molecular docking of selected inhibitors (**5e** and **6a**) into the active site cavities of X-ray crystallographic models of MAO-A and -B. The inhibitors (**5e** and **6a**) were drawn in Discovery Studio, hydrogen atoms were added according to the appropriate protonation states at pH 7.4 and the geometries were briefly optimized using a fast Dreiding-like forcefield (1000 iterations) available for this purpose in Discovery Studio. The atom potential types and partial charges were then automatically assigned with the Momany and Rone CHARMM forcefield.

The X-ray crystallographic structures of MAO-A in complex with harmine (PDB code: 2Z5X)<sup>41</sup> and MAO-B in complex with safinamide (PDB code: 2V5Z)<sup>42</sup> were acquired from the RCSB Protein Data Bank ([www.rcsb.org/pdb](http://www.rcsb.org/pdb)). Hydrogen atoms were added to the crystallographic structures according to the appropriate protonation states of the ionizable amino acids at pH 7.4. The valences of the FAD cofactors (oxidized state) and co-crystallized ligands (harmine and safinamide) were corrected, hydrogen atoms were added according to the appropriate protonation states at pH 7.4. The resulting models were automatically typed with the Momany and Rone CHARMM forcefield, the protein backbone was constrained and the models were subjected to a three step energy minimization cascade. The first step, a steepest descent minimization step was followed by a conjugate gradient minimization step. For both minimization steps the termination criteria was set to a maximum of 2500 steps or a minimum value of 0.1 for the root mean square of the energy gradient. The third step was an adopted basis Newton-Rapheson minimization step with the termination criteria set to a maximum of 5000 steps or a minimum value for the root mean square of the energy gradient of 0.01. For all steps of this minimization cascade the implicit generalized Born solvation model with simple switching was used with the dielectric constant set to 4. The co-crystallized ligands and backbone constraints were subsequently removed from the active sites of the MAO-A and -B crystallographic structures and the binding sites were identified by a flood-filling algorithm. The crystallized water molecules were also removed from the crystallographic structures with the

exception of 4 active site water molecules in both MAO-A and -B. Examination of the X-ray crystallographic structures of MAO-B have shown that three active site water molecules (HOH 1155, 1170 and 1351; A-chain) are conserved, all in the vicinity of the FAD cofactor.<sup>42</sup> Preliminary docking studies in our laboratory has also suggested that HOH 1346 (MAO-B, A-chain) may also be involved in stabilizing potential inhibitors within the active site and was thus also retained. For the docking studies with MAO-A, the crystal waters were also removed with the exception of HOH 710, 739 and 725 which occupies the corresponding positions in the MAO-A active site to those positions that are occupied in the MAO-B active site by the integral water molecules listed above. Docking was subsequently carried out with the LigandFit protocol of Discovery Studio. This protocol uses total ligand flexibility whereby the final ligand conformations are determined by the Monte Carlo conformation search method set to a variable number of trial runs. The docked ligands were further refined using in situ ligand minimization with the Smart Minimizer algorithm. All parameters for the docking runs were set to their default values and ten possible binding solutions were computed for each docked ligand. The best-ranked binding conformation of each ligand was determined according to the DockScore values. The illustrations were prepared in PYMOL.<sup>47</sup>

## Acknowledgments

NMR spectra were recorded by André Joubert of the SASOL Centre for Chemistry, North-West University while the MS spectra were recorded by Marelize Ferreira of the Mass Spectrometry Service, School of Chemistry, University of the Witwatersrand. Support with the HPLC analysis was provided by Jan du Preez from the Analytical Technology Laboratory, North-West University. This work was supported by grants from the National Research Foundation and the Medical Research Council, South Africa.

## Supplementary data

Supplementary data associated with this article can be found, in the online version, at [doi:10.1016/j.bmc.2011.06.070](https://doi.org/10.1016/j.bmc.2011.06.070).

## References and notes

- Binda, C.; Newton-Vinson, P.; Hubálek, F.; Edmondson, D. E.; Mattevi, A. *Nat. Struct. Biol.* **2002**, *9*, 22.
- Edmondson, D. E.; Mattevi, A.; Binda, C.; Li, M.; Hubálek, F. *Curr. Med. Chem.* **2004**, *11*, 1983.
- Shih, J. C.; Chen, K.; Ridd, M. J. *Annu. Rev. Neurosci.* **1999**, *22*, 197.
- Weyler, W.; Hsu, Y. P.; Breakefield, X. O. *Pharmacol. Ther.* **1990**, *47*, 391.
- Chen, K.; Wu, H. F.; Shih, J. C. *J. Neurochem.* **1993**, *61*, 187.
- Weyler, W.; Salach, J. I. *J. Biol. Chem.* **1985**, *260*, 13199.
- Saura, J.; Bleuel, Z.; Ulrich, J.; Mendelowitsch, A.; Chen, K.; Shih, J. C.; Malherbe, P.; Da Prada, M.; Richards, J. G. *Neuroscience* **1996**, *70*, 755.
- Inoue, H.; Castagnoli, K.; Van der Schyff, C. J.; Mabic, S.; Igarashi, K.; Castagnoli, N., Jr. *J. Pharmacol. Exp. Ther.* **1999**, *291*, 856.
- Westlund, K. N.; Denney, R. M.; Rose, R. M.; Abell, C. W. *Neuroscience* **1988**, *25*, 439.
- Fowler, J. C.; Wiberg, A.; Orelund, L.; Marcusson, J.; Winblad, B. *J. Neural Transm. Gen. Sect.* **1980**, *49*, 1.
- Kalaria, R. N.; Mitchell, M. J.; Harik, S. I. *Brain* **1988**, *111*, 1441.
- Collins, G. G. S.; Sandler, M.; Williams, E. D.; Youdim, M. B. H. *Nature* **1970**, *225*, 817.
- Waldmeier, P. C. *J. Neural Transm. Suppl.* **1987**, *23*, 55.
- Youdim, M. B. H.; Edmondson, D.; Tipton, K. F. *Nat. Rev. Neurosci.* **2006**, *7*, 295.
- Youdim, M. B. H.; Bakhle, Y. S. *Br. J. Pharmacol.* **2006**, *147*, S287.
- Singer, T. P.; Ramsay, R. R.; McKeown, K.; Trevor, A.; Castagnoli, N., Jr. *Toxicology* **1988**, *49*, 17.
- Zisook, S. E. *Psychosomatics* **1985**, *26*, 240.
- Youdim, M. B. H.; Collins, G. G. S.; Sandler, M.; Bevan-Jones, A. B.; Pare, C. M.; Nicholson, W. J. *Nature* **1972**, *236*, 225.
- Di Monte, D. A.; DeLanney, L. E.; Irwin, I.; Royland, J. E.; Chan, P.; Jakowec, M. W.; Langston, J. W. *Brain Res.* **1996**, *738*, 53.
- Finberg, J. P.; Wang, J.; Bankiewicz, K.; Harvey-White, J.; Kopin, I. J.; Goldstein, D. S. *J. Neural Transm. Suppl.* **1998**, *52*, 279.
- Fernandez, H. H.; Chen, J. *J. Pharmacotherapy* **2007**, *27*, 174S.
- Nicotra, A.; Pierucci, F.; Parvez, H.; Senatori, O. *Neurotoxicology* **2004**, *25*, 155.
- Fowler, J. S.; Volkow, N. D.; Wang, G. J.; Logan, J.; Pappas, N.; Shea, C.; MacGregor, R. *Neurobiol. Aging* **1997**, *18*, 431.
- Youdim, M. B.; Weinstock, M. *Neurotoxicology* **2004**, *25*, 243.
- Fowler, J. S.; Volkow, N. D.; Logan, J.; Wang, G. J.; MacGregor, R. R.; Schyler, D.; Wolf, A. P.; Pappas, N.; Alexoff, D.; Shea, C. *Synapse B* **1994**, *18*, 86.
- Hubálek, F.; Binda, C.; Khalil, A.; Li, M.; Mattevi, A.; Castagnoli, N., Jr.; Edmondson, D. E. *J. Biol. Chem.* **2005**, *280*, 15761.
- Binda, C.; Li, M.; Hubálek, F.; Restelli, N.; Edmondson, D. E.; Mattevi, A. *Proc. Natl. Acad. Sci. U.S.A.* **2003**, *100*, 9750.
- Van der Walt, E. M.; Milczek, E. M.; Malan, S. F.; Edmondson, D. E.; Castagnoli, N., Jr.; Bergh, J. J.; Petzer, J. P. *Bioorg. Med. Chem. Lett.* **2009**, *19*, 2509.
- Manley-King, C. I.; Bergh, J. J.; Petzer, J. P. *Bioorg. Med. Chem.* **2011**, *19*, 261.
- Galanin, N. E.; Kudrik, E. V.; Shaposhnikov, G. P. *Russ. J. Org. Chem.* **2006**, *42*, 603.
- Tau, P.; Nyokong, T. *Electrochim. Acta* **2007**, *52*, 3641.
- Pluempunap, W.; Adisakwattana, S.; Yibchok-Anun, S.; Chavasiri, W. *Arch. Pharm. Res.* **2007**, *30*, 1501.
- Novaroli, L.; Reist, M.; Favre, E.; Carotti, A.; Catto, M.; Carrupt, P. A. *Bioorg. Med. Chem.* **2005**, *13*, 6212.
- Strydom, B.; Malan, S. F.; Castagnoli, N.; Bergh, J. J.; Petzer, J. P. *Bioorg. Med. Chem.* **2010**, *18*, 1018.
- Prins, L. H. A.; Petzer, J. P.; Malan, S. F. *Eur. J. Med. Chem.* **2010**, *45*, 4458.
- Cheng, Y. C.; Prusoff, W. H. *Biochem. Pharmacol.* **1973**, *22*, 3099.
- Pretorius, J. P.; Malan, S. F.; Castagnoli, N., Jr.; Bergh, J. J.; Petzer, J. P. *Bioorg. Med. Chem.* **2008**, *16*, 8676.
- Vlok, N.; Malan, S. F.; Castagnoli, N., Jr.; Bergh, J. J.; Petzer, J. P. *Bioorg. Med. Chem.* **2006**, *14*, 3512.
- Petzer, J. P.; Steyn, S.; Castagnoli, K. P.; Chen, J. F.; Schwarzschild, M. A.; Van der Schyff, C. J.; Castagnoli, N., Jr. *Bioorg. Med. Chem.* **2003**, *11*, 1299.
- Iley, J.; Calheiros, T.; Moreira, R. *Bioorg. Med. Chem. Lett.* **1998**, *8*, 955.
- Son, S.-Y.; Ma, J.; Kondou, Y.; Yoshimura, M.; Yamashita, E.; Tsukihara, T. *Proc. Natl. Acad. Sci. U.S.A.* **2008**, *105*, 5739.
- Binda, C.; Wang, J.; Pisani, L.; Caccia, C.; Carotti, A.; Salvati, P.; Edmondson, D. E.; Mattevi, A. *J. Med. Chem.* **2007**, *50*, 5848.
- Binda, C.; Angelini, R.; Federico, R.; Ascenzi, A.; Mattevi, A. *Biochemistry* **2001**, *40*, 2766.
- Binda, C.; Mattevi, A.; Edmondson, D. E. *J. Biol. Chem.* **2002**, *277*, 23973.
- Novaroli, L.; Daina, A.; Favre, E.; Bravo, J.; Carotti, A.; Leonetti, F.; Catto, M.; Carrupt, P. A.; Reist, M. *J. Med. Chem.* **2006**, *49*, 6264.
- Sou, S.; Mayumi, S.; Takahashi, H.; Yamasaki, R.; Kadoya, S.; Sodeoka, M.; Hashimoto, Y. *Bioorg. Med. Chem.* **2000**, *10*, 1081.
- DeLano, W. L. *The PyMOL Molecular Graphics System*; DeLano Scientific: San Carlos, USA, 2002.